

# Spider Diagram for Tubular Expansion with Restraints

F Marketz<sup>a</sup> and SA Al-Hiddabi<sup>\*b</sup>

<sup>a</sup>Lead Production Technologist, Maersk Oil, Copenhagen, Denmark

<sup>b</sup>The Research Council of Oman, Muscat, Sultanate of Oman

Received 22 April 2012 ; accepted 26 November 2012

**Abstract:** The aim of this study is to explain the mechanics of tubular expansion in irregularly shaped boreholes such as those frequently observed in the upper Natih reservoirs. Statistical analysis of borehole data does not indicate a strong correlation between the non-circularity and expanded tubular's in such boreholes. A two-dimensional (2-D) finite element model was developed using commercial software to determine the non-circularity of an expanded tubular and those data were compared with the measured values. A parametric study was also conducted and spider plots were generated to determine the amount of irregularity in the expanded tubulars so that optimum operational parameters could be identified to limit cross-section irregularities during the expansion process.

**Keywords:** Tubular expansion, Irregular boreholes, Spider diagram, Finite element analysis

## مخطط عنكبوتي لوصف عملية تمديد أنابيب الآبار في وجود عوائق

فرانز ماركتز<sup>أ</sup> وسيف ع الهدابي<sup>ب\*</sup>

**الملخص:** تهدف هذه الدراسة إلى فهم آليات عملية تمديد الأنابيب في الآبار غير المنتظمة الشكل مثل تلك الموجودة في خزانات نطيج العليا. حيث أوضحت نتائج تحليل البيانات الإحصائية للآبار عدم وجود علاقة قوية بين عدم انتظام دائرية البئر وتمديد الأنابيب في مثل هذه الآبار. ولدراسة ذلك فقد تم تطوير نموذج ثنائي الأبعاد باستخدام أحد البرامج الهندسية التي تعتمد على طريقة العنصر المحدود وذلك من أجل تحديد مقدار عدم الانتظام في دائرية الأنبوب الممدد، ثم مقارنة النتائج المنبثقة مع القيم المأخوذة بالقياس المباشر. كما تم أيضا إجراء دراسة تحليلية للعديد من العوامل المؤثرة على هذه العملية، وبناء على ذلك فقد تم إنشاء مخططات عنكبوتية لتحديد مقدار عدم الانتظام في الأنبوب الممدد حتى يتسنى تحديد العوامل التشغيلية المثلى للحد من عدم انتظام المقطع العرضي للأنبوب خلال عملية التمديد.

**المفردات المفتاحية:** تمديد الأنابيب، آبار غير منتظمة، مخطط عنكبوتي، التحليل بطريقة العنصر المحدود.

## 1. Introduction

The redevelopment of a major brown field requires a careful selection of the right recovery mechanisms for the target fractured carbonate reservoirs. Additionally, low-cost well delivery with conformance control through implementation of new technologies is desirable. Drilling through fractured reservoir sections can cause drilling losses that must be cured in order to place cement in the annulus. Over the past 30 years, liner cementation in wells with severe or heavy drilling losses has had limited success despite many innovations in loss curing and liner cementation meth-

ods. Therefore, expandable tubular and swelling elastomer sealing technologies have been introduced for water flood appraisal drilling as an alternative to cemented liners. This has been done to provide zonal isolation, which is critical for profile control; eliminate the need for curing losses and liner cementation, and slim well design, or reduce the size of the top hole in order to reduce the "footprint". In this study, both vertical oil producers and water injectors were drilled with losses and lined with expandable tubular shafts over the reservoir section. Elastomer seals isolated the

\*Corresponding author's e-mail: hiddabi@trc.gov.om

the multiple reservoirs from one another. Expandable tubular technology has enabled a slimmer oil production design, thereby allowing the creation of zonal isolation without the use of cement: elastomer seals are energized between the expanding tubular shaft and its formation during expansion. Similarly, the use of open-hole liners is based on expanding a liner across an open-hole section and into the previous tubular to form a liner hanger. Elastomer seals on the outside provide enhanced capability for zonal isolation in the open-hole design; hence, the open-hole liner expands against the formation to create a seal and then the elastomers swell when they come into contact with water in order to improve the sealing.

The technology of down-hole tubular expansion provides cost-effective solutions to several well design and delivery problems which previously were obstacles to comprehensive reservoir exploitation. This technology has gained momentum and attracted the attention of operators and researchers as a common element in enhancing the economics and performance of both new and old wells. For example, secondary oil recovery is often impaired by zones of high permeability such as fractures, fault-related fracture corridors, and karstified parts of the reservoir (Fokker *et al.* 2005; Marketz *et al.* 2005; Lighthelm *et al.* 2006; Pervez *et al.* 2008). This impairment occurs primarily because of early water breakthrough through these zones from injectors to producers, as well as by uneven sweep of the formation. These zones can span from an aquifer to the wellbore, often resulting in water being cycled without any improvement in oil production (Ozkaya and Richard 2006). In order to avoid these problems, the down-hole closure of the fractures is developed using tubular expansion technologies with or without elastomer annular seals. This can be a non-invasive or invasive technique and, depending on the use of elastomers, has been applied in several wells with a water reduction rate of up to 40% and oil gains of up to 45 cubic meters per day per well (Welling *et al.* 2007). The recent observation of the resultant irregular cross-section after tubular expansion has posed new challenges to drilling completion. The tubular cross-section was not circular at different depths and at places become greater than the mandrel diameter. The tubular has to be milled to be able to run a packer, resulting in reduced tubular strength after expansion. This milling also results in reduced burst and collapse strength, making it susceptible to failure due to buckling. This phenomenon is believed to occur due to an expansion in irregularly shaped boreholes, thereby creating point loads between the expanding tubular and the formation during expansion. The only literature available on this phenomenon is that of (Akgun *et al.* 1994; Pervez and Qamar 2011).

Tubular expansion under restraint conditions occurs due to the presence of certain formations and results in varying diameters along the tubular axis. The minimum inside diameter of the expanded liner was smaller than the outside diameter of the expansion cone. The liner had to be milled to be able to run a packer. This is a phenomenon which has never been observed under normal circumstances and may have occurred due to expansion in a restrained space caused by the collapse of a drilled borehole. This can result in additional loading on to the tubular in addition to the normal expansion load. The major disadvantage is the reduction in clear space available for other equipment to be lowered down the hole to complete the well for production.

The main objective of this work is to understand the mechanics of tubular expansion in restrained boreholes, which are frequently observed in the upper Natih reservoirs. The minimum inner diameter of an expanded tubular pipe can be smaller than the drift diameter due to expansion in restrained boreholes. This prevents completion equipment from being run successfully. Finite element models of tubular expansion with and without elastomer seals in restrained boreholes were developed to determine the variations in contact pressure and displacements with respect to expansion ratios. These will assist in understanding the true mechanics of expansion in such boreholes.

## 2. Problem Formulation

Very little is available in the literature to explain the phenomenon of irregular tubular expansion. Currently, tubes are expanded either by pushing the cone hydraulically from the bottom up or by mechanically pulling the cone upward. The cross section of the expansion cone is circular; hence, it is expected that the expanded tubular cross section will also be circular. In most cases, they are circular but eccentric along the tubular length (*ie.* the centers of the circular sections at different depths do not lay on the same vertical line). However, in a few instances the well bore log data showed that the cross section of the expanded liner was non-circular at different depths, particularly in the upper Natih reservoirs. Because of this, the inner cross-section of the expanded tubular cannot be defined using one diameter. One will need a minimum of two dimensions at each cross section of importance to understand the expansion in a restrained borehole. This will also result in a variable thickness along the tubular axis, which may cause unexpected premature failure of the tubular. To avoid this, one must understand the reasons why it might happen as well as the circumstances surrounding failure. The irregularity in tubular diameter after expansion may happen for two reasons. First, if the borehole is itself not circular at

certain sections, then there will be restricted space for expansion of the tubular. As a result, point loads will act on the tubular shaft due to the complex boundary conditions. This will allow the tubular to expand more in one direction as compared to other directions once the expansion cone passes through it. As a result, the cross-section of that section will become non-circular. Second, the elastomer seal around the tubular is compressed against the formation as a result of the expansion process. Due to the elasticity of the elastomer and the properties of formation, elastic reaction forces will act on the expanded section of the tubular. This force will not be of the same magnitude along the circumference of the tubular. Hence, the tubular may become irregularly shaped after the expansion process.

A solid expandable tubular (SET) was installed in the borehole of a typical well. Later, the liner had to be milled to run a packer. The caliper data of this borehole and the installed expanded tubular were taken as the starting point. First, using the caliper data of the borehole and SET, the difference between the minimum and maximum diameters was calculated at various depths along the tubular's length. Statistical analysis was carried out to find any correlation between irregular expansion of the SET and the borehole. Second, a 2-D plane strain finite element model was developed using a general purpose finite element code ABAQUS/Explicit to model the expansion of tubular in a irregularly shaped borehole. Spider plots were generated to show the difference in extreme diameters of the SET section as a function of the expansion ratio, the tubular diameter, and the friction coefficient. The expansion ratio is defined using the expansion cone and pre-expanded tubular diameters as follows:

$$\text{Expansion ratio} = \frac{\text{OD}_{\text{Cone}} - \text{ID}_{\text{Pre-expanded tubular}}}{\text{ID}_{\text{Pre-expanded tubular}}} \times 100$$

A parametric study was conducted and contact pressure and displacements were plotted as a function of the expansion ratio.

### 3. Statistical Analysis

Correlation is a bivariate measure of the association (strength) of the relationship between two variables.

It varies from 0, indicating a random relationship, to 1 which indicates a perfect linear relationship, to -1,

which indicates a perfect negative linear relationship. Using the caliper data, the borehole irregularity (HOV) and expanded tubular diameter irregularity (POV) were calculated using Statistical Package for the Social Sciences (SPSS), version 20 software. The data are available from a depth of 330 meters to 593.9568 meters at varying intervals. In addition, the borehole data were recorded at smaller intervals as compared to the expanded tubular. A MATLAB code was written to read the data from an Excel datasheet at an interval of 1.65 centimeters through the depth. A 3-D scatter plot of the variables under investigation is shown in Fig. 1. It can be observed that there exists a relationship between depth, HOV, and POV. The data appear to be clustered around an observed path. The correlation between the three variables also has been investigated using SPSS. The results are shown in Table 1. A correlation coefficient of -0.738 indicates a strong relation between depth and hole irregularity whereas it is weak between depth and tubular irregularity as indicated by a correlation coefficient of 0.110. The direct relationship between expanded tubes and borehole irregularity is relatively weak, having a correlation coefficient of -0.200.

Figures 2 and 3 show the scatter plots of borehole and diametral irregularity of an expanded tubular shaft along depth of Natih reservoirs. It is obvious from Fig. 2 that the average borehole irregularity in the Natih B and Natih C1 reservoirs is 0.09 and 0.05 meters, respectively. However, the average values decreased to 0.01 meters starting from the Natih C2 reservoir. This is due to the different properties of the Natih reservoirs-the deeper they are the more consolidated they become. Figure 3 shows the irregularity in expanded tubular diameter at the Natih reservoirs' different depths. It has definite spikes, indicating large values in the Natih C1, C2, D1, and F1 reservoirs as compared to the rest of the Natih reservoirs. The magnitude of these irregularities at spike locations is much larger than other locations. These can be attributed to tight spots in the reservoir.

In this analysis, the direct tubular size ( $R_{\text{major}} - R_{\text{minor}}$ ) and caliper hole size ( $|\text{CAL}_1 - \text{CAL}_2|$ ) were used as the field variables to investigate the diameter irregularity phenomenon. The analysis would be more representative of actual configuration if the targeted hole-size (cone outer diameter) and actual SET size were used. Inclusion of the formation type or one of its representatives like modulus of elasticity in conjunction

**Table 1.** Correlation coefficients

	Depth	HOV	POV
Depth	1.000	-0.738	0.110
HOV	-0.738	1.000	-0.200
POV	0.110	-0.200	1.000

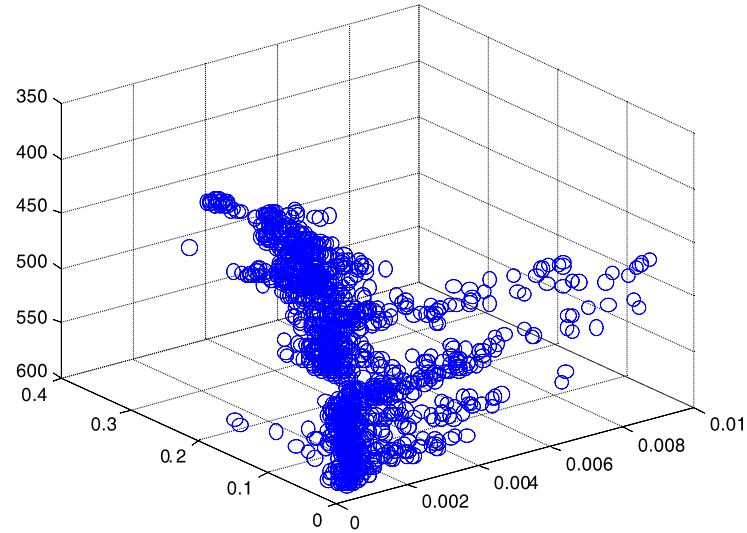


**Figure 1.** 3-D scatter plot showing HOV and POV at different depths

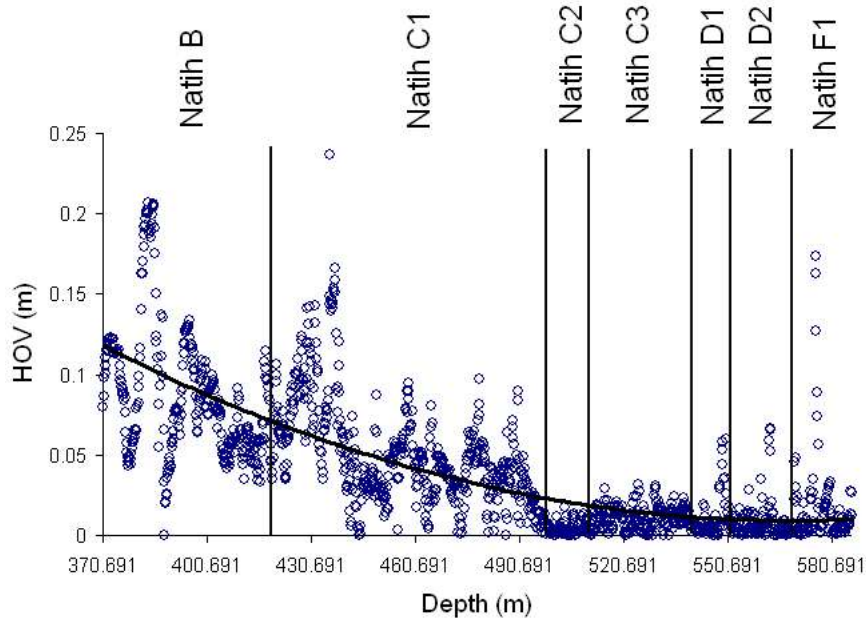


**Figure 2.** Scatter plot of variation in HOV along borehole depth

with borehole depth might lead to some conclusions of practical use. Using the existing data, the variation in the SET diameter irregularity with respect to the borehole diametral irregularities is plotted as shown in Fig. 4. For irregularities in large-size boreholes, there is no correlation with that of expanded tubular segments. For irregularities in small-size boreholes, there is a weak correlation with that of expanded tubular sections. Hence, it can be concluded that there is no or weak correlation between HOV and POV. Therefore, modeling and simulation of tubular expansion in an irregularly shaped borehole is required in order to have a clear understanding of the problem.

#### 4. 2-Dimensional Modeling

A 2-D model of tubular expansion against formation (borehole) was simulated using the finite element method. The depth of the tubular under consideration was much larger as compared to the planar dimensions of the tube and formation. Therefore, a plane-strain model of the two has been appropriately simplified from 3-D to 2-D. The model was developed by building up the geometry of the tubular and the rigid formation, inputting their corresponding material properties and imposing appropriate boundary conditions. Figure 5 shows the geometric model of tubular expansion.

Spider Diagram for Tubular Expansion with Restraints

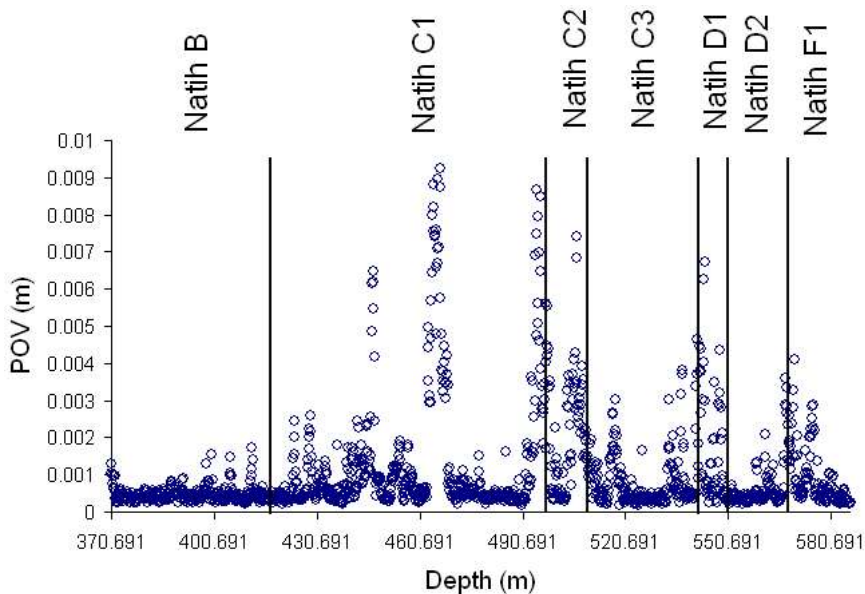


**Figure 3.** Scatter plot of variation in POV along borehole depth

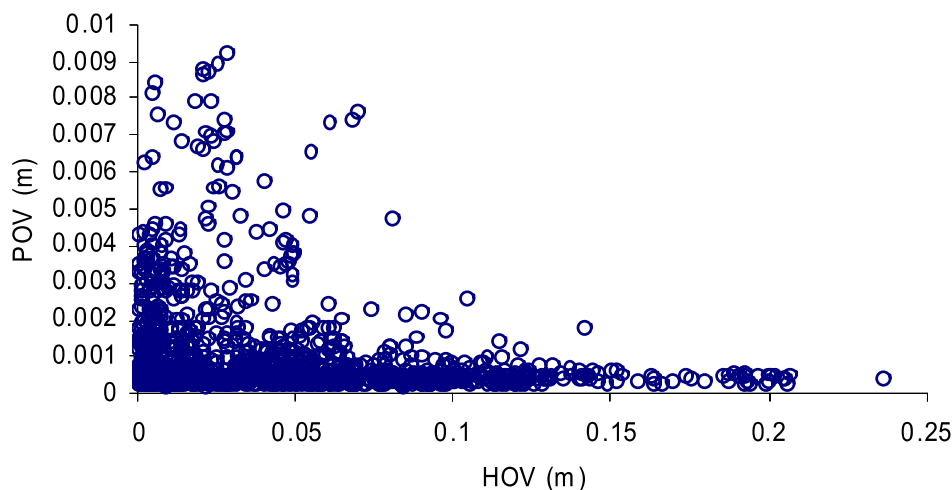


**Figure 4.** Scatter plot of variation in POV with respect to HOV

sion with the rigid formation. The tube-formation interface was modeled using the user-defined friction law to account for the induced friction between the interacting surfaces. Two different cases should be considered depending on the mechanistic behavior of the formation.

- \* Case-I: The formation was modeled as a rigid body. In this case, simulations could not be carried out for large expansion ratios due to the rigid formation.
- \* Case-II: The formation was modeled as linear elastic material.

The formation thickness for Case-I is immaterial for simulation due to the rigid body assumption. For

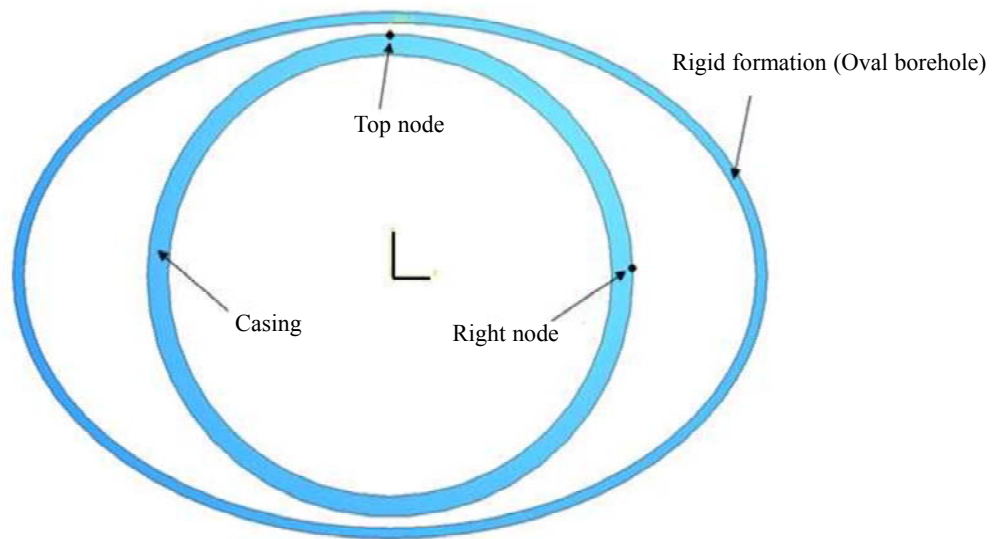
Case-II, the formation thickness was taken into consideration. Each run consisted of two distinct steps. In step one, the inner surface of the tube was allowed to expand by prescribing radial displacements up to the final expansion ratio. In step two, the displacements were released to establish free equilibrium, which is a term used in ABAQUS to define the equilibrium under no load. The resultant displacement, stresses, strains, and deformed configurations were analyzed to determine the causes of ovality. Simulation results were obtained at nodes as shown in Fig. 5. Two different solid expandable tubular systems were used for the simulation. The tube's pre-expansion outer and inner diameters (OD and ID, respectively), material properties, and borehole diameter are given in Table 2. The formation properties for the Natih reservoir are given in Table 3.

**Table 2.** Geometry and material parameters for the tubes

OD (mm)	ID (mm)	Borehole (mm)	Expansion Ratio	E (GPa)	Yield (MPa)
139.70	124.26	157.07	10.6 %	208	595
139.70	124.26	163.98	16.1%	208	595
193.68	174.63	224.86	16.1%	208	595

**Table 3.** The formation properties of the Natih reservoir

Young's modulus	7.5 GPa
Poisson's ratio	0.2
Cohesion	7.515550 MPa
Friction Angle	18 deg
Dilation Angle	15 deg

**Figure 5.** Geometrical model of tubular expansion in an oval borehole against rigid formation (Case-I)

It is important to observe the way the contact conditions develop between the tubular and the formations during the expansion process, which will help to determine the possible causes of irregularity in expansion. Figure 6 shows the variation in contact pressure between the tubular and rigid formations for 7 and 10% expansion ratios. In a rigid formation, the contact pressure increased by 100%, for a small increase of 3% in the expansion ratio. However, for an elastic formation (Case-II), the magnitude of contact pressure, in general, is approximately 10% lower than that of the rigid formation (Case-I) as shown in Fig. 7. It is obvious from the spider diagrams of Figs. 6 and 7 that contact pressure increases significantly when formation is more consolidated.

It was observed that the large surface contact in the beginning between tubular and the geological formation later changed to two small regional contacts (limit to a point) once equilibrium was established as shown in Fig. 8. During this contact, the resultant reaction

forces at the inner surface of the tubular forced a change in direction as well as magnitude near the end of the contact region between the tubular and the formation. This resulted in a two-point curved bending at and around the contact region. Hence, the complete tubular had been subjected to loads at four locations (two each at the top and bottom) resulting in a non-circular shaped expansion. The amount of non-circularity in the expanded tubular can be determined by subtracting displacement values at the top and right side nodes.

The equivalent plastic strains increased gradually for both the top and right side nodes at the beginning of expansion and then remained constant until the initiation of contact. Later, there was a significant increase in equivalent plastic strain at the top node as compared to a negligible increase for right side node. Table 4 shows the equivalent plastic strain at the top node for different expansion ratios. It is clear from the table that the magnitude of plastic strain increased

## Spider Diagram for Tubular Expansion with Restraints

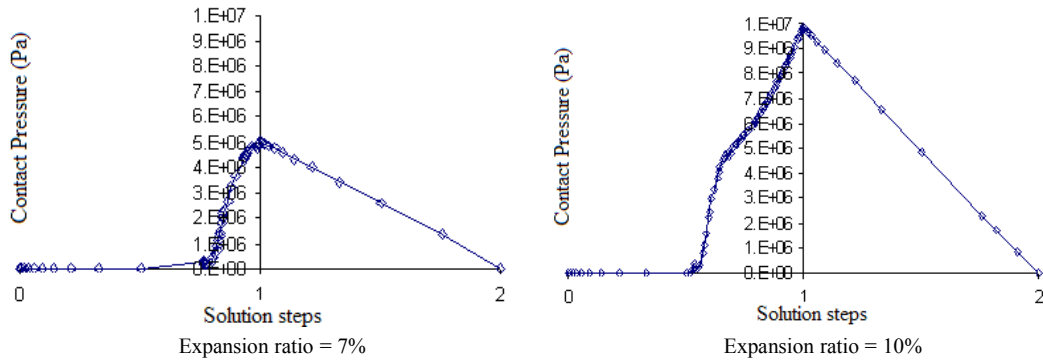


Figure 6. Variation in contact pressure at different expansion ratios for Case-I

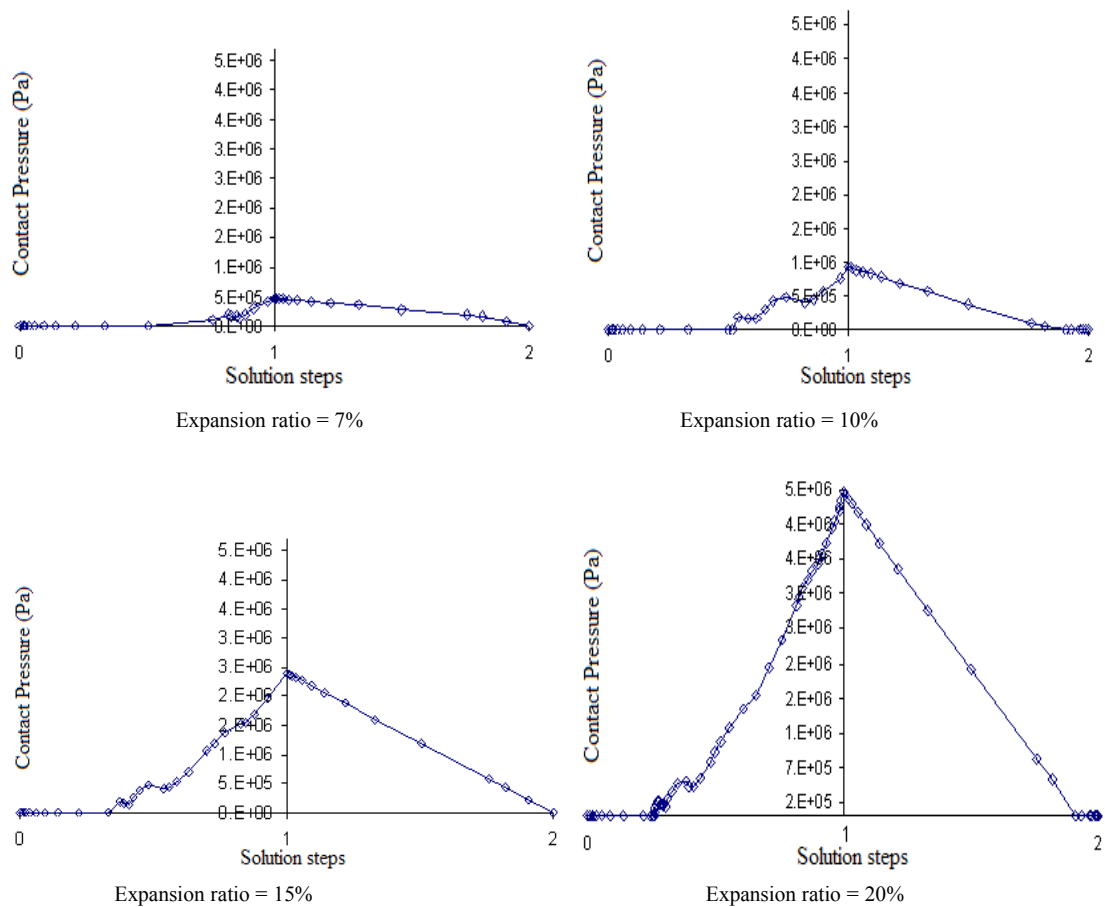


Figure 7. Variation in contact pressure at different expansion ratios for Case-II

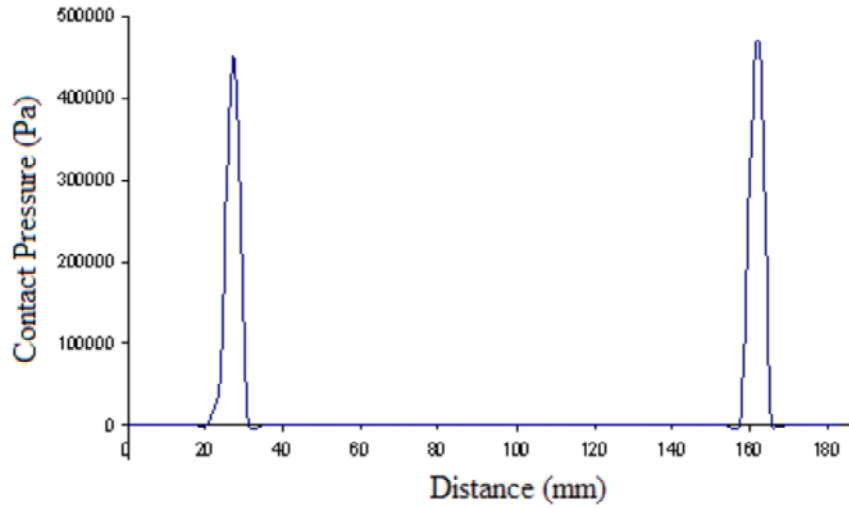
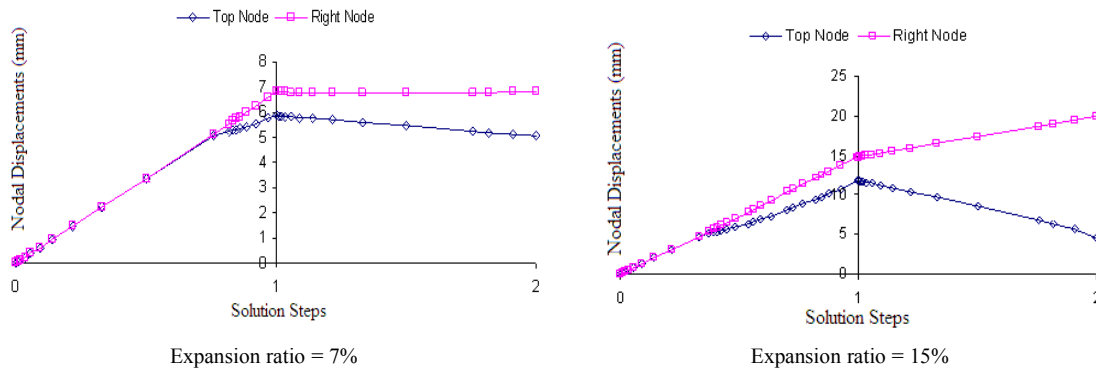
drastically for expansion ratios of 10% and above. The large magnitude of equivalent plastic strain was due to excessive radial plastic deformation at the right side nodes originating from severe constraints at the top and bottom contact regions. This behavior was observed for both cases and at all expansion ratios. However, non-linearity was much more prominent in Case-II.

The von Mises effective stress behaved in a similar manner to the equivalent plastic strain except that,

after contact initiation, the stress increased at the top node and decreased at right side node. The right side node was free to expand and hence experienced stresses to a lesser degree. The displacement of both nodes increased linearly until the tubular came in contact with the formation. Afterwards, the right side node continued to deform due to the absence of constraints, while the top node deformed negligibly depending on the elasticity of the formation. The displacement at these nodes for both cases at various expansion ratios is shown as spider diagram in Fig. 9.

**Table 4.** Variation in equivalent plastics strain w.r.t expansion ratio (Case II)

Expansion Ratio	Equivalent Plastic Strain ( $\varepsilon_p^{Top Node}$ )
7%	22.3%
10%	44.2%
15%	61.4%
20%	68.1%

**Figure 8.** Contact pressure against elastic formation at the end of step two**Figure 9.** Nodal displacement variation with solution steps for Case-II

The irregularity in diameter obtained from the simulation was compared with the value calculated using the actual well data provided. The caliper data yielded an average irregularity of 3.5 mm while the simulation result for Case-II gave a 2.55 mm irregularity, in simulation. In addition, the bending in the vicinity of the top node resulted in excessive necking in a no-contact region. Under this circumstance, it is not possible to calculate the irregularity in the diameter of the expanded tubular segment. This was the case for many expansion ratios, which occurred due to the oversimplification of the expansion process. Also, the axial deformation of the tubular was ignored in the 2-D plane strain analysis. Therefore, the limitations of the plane-strain

model have led us to regard the tubular expansion process as a 3-D problem.

Before embarking on 3-D analyses, a generalized plane strain model (GPE) was developed to check whether it would yield accurate results without the extensive computational resources required for a 3-D analysis. The generalized plane strain theory used in ABAQUS assumes that the model lies between two bounding planes which may move as rigid bodies with respect to each other, thus causing strain of the thickness direction fibers of the model. It is assumed that the deformation of the model is independent of position with respect to this thickness direction, so the relative motion of the two planes causes a direct strain on



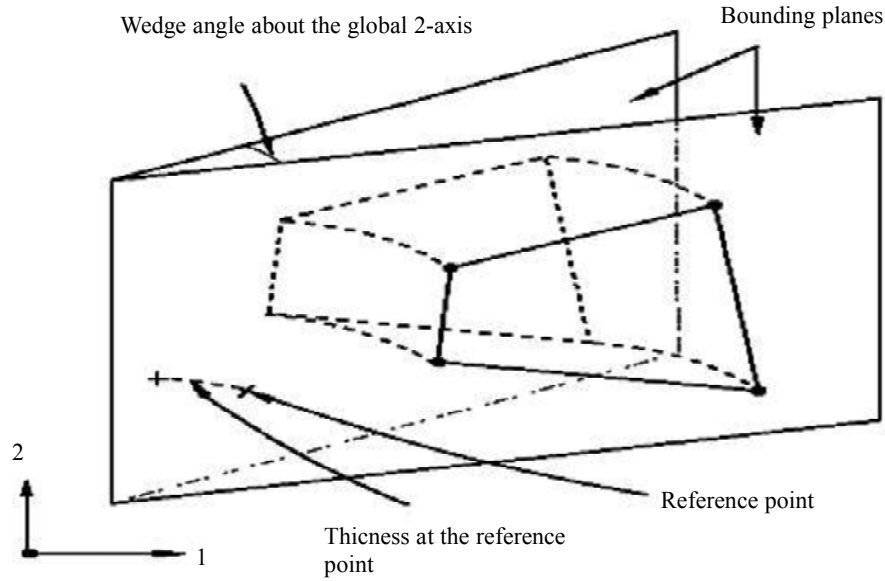


Figure 10. Defining generalized plane strain element in ABAQUS

$$\begin{array}{c}
 \begin{bmatrix} \sigma_{rr} & \sigma_{r\theta} & \sigma_{rz} \\ \sigma_{r\theta} & \sigma_{\theta\theta} & \sigma_{\theta z} \\ \sigma_{rz} & \sigma_{\theta z} & \sigma_{zz} \end{bmatrix} \\
 \text{Stress tensor}
 \end{array}
 \longrightarrow
 \begin{array}{c}
 \begin{bmatrix} -106.86 & 1.11 & 0.0 \\ 1.11 & -1.06 & 0.0 \\ 0.0 & 0.0 & 50.68 \end{bmatrix} \\
 \text{Top node}
 \end{array}
 \quad \& \quad
 \begin{array}{c}
 \begin{bmatrix} -1.36 & 1.41 & 0.0 \\ 1.41 & -98.4 & 0.0 \\ 0.0 & 0.0 & -147.2 \end{bmatrix} \\
 \text{Right side node}
 \end{array}$$

Figure 11. Stress tensor (MPa) at top and right side nodes after expansion

the thickness direction fibers only. A reference point to indicate the reference node required by the generalized plane strain elements was created in the model. Generalized plane strain sections were used to define the section properties of 2-D planar regions. In addition to the material and section thickness at the reference point, the wedge angles about the global 1- and 2-axes are as defined in Fig. 10.

The stress tensors at top and right side nodes after expansion are shown in Fig. 11. It is obvious that, after expansion, shear stresses are negligible. Axial stresses at both nodes were equal to 50% and 150% of the radial and circumferential stresses respectively. This clearly indicates that a simplified plane strain model is not an appropriate model. The maximum effective stress occurred on the outer surface near the right side's region. The magnitude was 297 MPa, which was half of the material yield strength. Hence, the tubular would not experience any post-expansion local failure. The GPE finite element analysis resulted in an irregularity of 3.65 mm resulting in less error compared to measured values. The results were definitely better than those obtained in the plane strain model, and the error may reduce further when a 3-D model is used.

## 5. Conclusions

A study was conducted to understand the tubular expansion in irregularly shaped boreholes such as those frequently observed in the upper Natih reservoirs using 2-D finite element analysis. Prior to FE analysis, efforts were made to develop correlations based on well caliper data. Two separate statistical packages were used to determine from circular cross-sections the correlation between borehole and tubular variations in the diameter. The available data did not yield any correlation. However, there were large irregularities in Natih reservoirs C1, C2, D1 and F1 as compared to the rest of the Natih reservoirs due to tight spots in those reservoirs. The major cause of the irregular shape of the expanded tubes is the restricted expansion of the tubular in the borehole at few locations. When tubular's come in contact with formations at these locations, reaction forces get activated, resulting in a 2-point to 4-point inward bending of the tubular section in the vicinity of the contact region. This also results in a higher deformation in those sections of the tubular which were not restricted in expansion. This whole process resulted in minor to major irregu-

lar expansion of the tubes. A 2-D finite element analysis captured the irregular expansion of the tubes but was not able to predict it accurately. Both plane strain model and generalized plane strain model were used for analysis. The predicted ovality had an error of 27% for the plane strain model and 21% for the generalized plane strain model when compared to measured irregularities. The 2-D model ignores the expansion effect in the axial direction, which turns out to be the limiting factor in this analysis. The influence of plastic formation properties is noticeable on the non-circularity of expanded tubular's. Considering a formation as pure elastic material results in higher variations in the tubular diameter.

## References

- Akgun F, Mitchell, BJ, Huttelmaier HP (1994), API tubular ovality and stresses in horizontal wells with finite element method. *SPE Drilling and Completion* 9:103-106.
- Fokker PA, Verga F, Egberts PJP (2005), New semi analytic technique to determine horizontal well productivity index in fractured reservoirs. *SPE Reservoir Evaluation Engineering* 8(1):123-131.
- Lighthelm DJ, Hoek PJ, Hos P, Faber MJ, Roeterdink RC (2006), Improved oil recovery in fractured carbonate reservoirs: Don't give induced fractures a chance. *SPE paper 98386. SPE Europe/EAGE Conference, Vienna, 12-15 June.*
- Marketz F, Leuranguer C, Welling RWF, Ogoke V (2005), Waterflood appraisal-Well delivery with expandable tubular. Paper # IPTC-10345. *International Petroleum Technology Conference, Doha, Qatar, 21-23 November.*
- Ozkaya SI, Richard PD (2006), Fractured reservoir characterization using dynamic data in a carbonate field. *SPE Reservoir Evaluation Engineering* 9(3):227-238.
- Pervez T, Qamar SZ, Seibi A, Al-Jahwari FK (2008), Use of SET in cased and open holes: Comparison between aluminum and steel. *Journal of Materials and Design* 29:811-817.
- Pervez T, Qamar SZ (2011), Finite element analysis of tubular ovality in oil well. *Advanced Materials Research* 264-265:1654-1659.
- Welling RWF, Marketz F, Moosa R, Riyami N, Follows EJ, Bruijn G, Hosny K (2007), Inflow profile control in horizontal wells in a fractured carbonate using swellable elastomers. *SPE paper # 105709. 15th SPE Middle East Gas Show and Conference, Bahrain, 11-14 March.*